Running with Flapping Wings

Kevin Peterson
Ronald S. Fearing, Ed.
Robert Full, Ed.

Electrical Engineering and Computer Sciences
University of California at Berkeley

Technical Report No. UCB/EECS-2010-76
http://www.eecs.berkeley.edu/Pubs/TechRpts/2010/EECS-2010-76.html

May 14, 2010

Acknowledgement

The author would like to thank Ron Fearing for all of his assistance and guidance on this work, and Robert Full for the many discussions and suggestions for improving the results. Great thanks to Paul Birkmeyer for the use of DASH as a starting platform for this research, as well as the many design discussions and ideas generated, and to Ankur Mehta, for the use of the GINA mote. Finally, thank you to all of my colleagues in the Biomimetics Millisystems Lab for all of your comments and suggestions throughout the course of the work.

Running with Flapping Wings

by Kevin C. Peterson

Research Project

Submitted to the Department of Electrical Engineering and Computer Sciences, University of California at Berkeley, in partial satisfaction of the requirements for the degree of **Master of Science, Plan II**.

Approval for the Report and Comprehensive Examination:

Committee:

Ronald Fearing
Research Advisor

Date

* * * * * *

Robert Full
Second Reader

Date

Abstract

Running with Flapping Wings

by

Kevin C. Peterson

Master of Science in Electrical Engineering

University of California, Berkeley

Ronald Fearing, Advisor

DASH+Wings is a small hexapedal winged robot derived from the Dynamic Autonomous Sprawled Hexapod (DASH). Drawing inspiration from nature, DASH+Wings uses wing assisted running to enable increased mobility. It shows a great improvement over DASH in its ability to traverse smooth inclines. To understand the differences in the motion of DASH and DASH+Wings, they are fitted with the GINA mote, a small electronics package that contains a processor, IMU, and radio. The acceleration, velocity and position profile as the robots are running can be compared, and the differences in motion quantified. The accelerometer data can also be used to classify good versus poor running performance, and assist with proper tuning of the system.

Contents

List of Figures **iii**

1 Introduction **1**

2 Design **4**
2.1 DASH - Dynamic Autonomous Sprawled Hexapod 4
2.2 Hybrid Locomotion - DASH+Wings 6
2.3 Accelerometer Integration 8
2.4 PID Motor Control 9
2.5 Compliant Foot Design 10

3 Methods **13**
3.1 Data Conditioning 14
3.2 Open Loop Synchronization 15
3.3 Closed Loop Synchronization 18

4 Results **20**
4.1 Incline running 20
4.2 Level Running 22
4.3 Hop Gait 29

5 Discussion and Conclusions **35**

Bibliography **40**

List of Figures

1.1 DASH+Wings 2

2.1 Differential drive motion of the top and bottom plates of DASH 5
2.2 Attachment of wings to DASH 7
2.3 Electronics package 8
2.4 Compliant leg design 12

3.1 Spline approximation of data 15
3.2 Back EMF signal with fixed PWM duty cycle and PID velocity control . . . 16
3.3 Parameterizing the acceleration signal 17
3.4 Determination of the back EMF scale factor using correlation 19

4.1 Incline Running 21
4.2 Measured accelerations of DASH in free-fall 24
4.3 Measured accelerations of DASH, with stride events marked 25
4.4 Measured accelerations of DASH+Wings, with stride events marked 26
4.5 Comparison of the acceleration over a single motor cycle between DASH and DASH+Wings 27
4.6 Comparison of the velocity over a single motor cycle between DASH and DASH+Wings 28
4.7 Comparison of the trajectories over a single motor cycle between DASH and DASH+Wings 30
4.8 Running with a hopping gait 31
4.9 Acceleration pattern for a hopping gait, correlated with a one cycle and two cycle period 32
4.10 Motion of a hopping gait compared to a smooth gait 33

Chapter 1

Introduction

The varied environments one finds outside of the laboratory often present unique and difficult challenges for the locomotion of small robots. Ground based robots may find themselves confronted with obstacles they cannot go over or around, while unsteady airflows can cause an aerial robot to crash. Legged locomotion allows robots such as RHex [1] to traverse complicated terrain, and ornithopters have been built that take advantage of the maneuverability of flapping flight for aerial locomotion [2]. However, a hybrid robot capable of both aerial and terrestrial locomotion offers the ability to choose the transport mode that is most advantageous at the time. Improving the locomotion capabilities of small robots is important for them to succeed in real world environments. Even small improvements in locomotion can allow for greatly increased mobility, before full hybrid locomotion is achieved. Through the study of intermediate modes of motility, design improvements can be made that will enable a robot to become capable of fully hybrid locomotion.

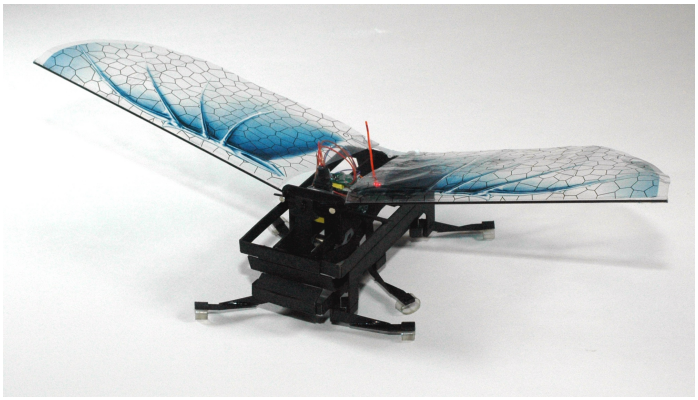

Figure 1.1: DASH+Wings, a dynamic hexapedal flapping winged robot.

There are many biological examples of incremental improvement in locomotion. One such example is wing assisted incline running (WAIR) exhibited by several precocial species of birds [3] [4]. Before they are capable of aerial flight, new hatchlings have been shown to use their wings for both ascending inclined surfaces as well as for controlled descent. In fact, adult birds capable of aerial flight often choose to run up sloped surfaces using WAIR instead of simply flying to the top. The first winged dinosaurs were thought to have used their wings primarily for thrust generation, increasing their horizontal velocity and ability to jump to large distances [5], improving their chances of survival.

This thesis introduces DASH+Wings, a small hexapedal robot capable of wing assisted running. Derived from the Dynamic Autonomous Sprawled Hexapod, or DASH [6], a single motor and transmission are used to drive the six legs and two wings. DASH+Wings also uses the scaled Smart Composite Manufacturing (SCM) process [7] used by DASH, allowing for fast build times and easily modified designs. The robot is 10 cm long, with a wing

span of 30 cm and a mass of 21.4 grams. The addition of wings to DASH allows for increased locomotion abilities on terrains that the original version of DASH finds impassable. To study the effects of flapping wings on horizontal locomotion, DASH and DASH+Wings are fitted with a small accelerometer allowing the measurement of the accelerations during the course of a stride. Previous studies have looked at the ground reaction forces of crawling robots [6], as well as the effects of simple flapping wings [8] during aerial flight. In a running robot these forces are coupled through the friction forces at the feet and cannot be considered independently. In addition, when running close to the ground the aerodynamic forces are enhanced due to ground effect. By comparing the different locomotion patterns of DASH and DASH+Wings, the aerodynamic and inertial effects of the wings can be determined.

Chapter 2

Design

DASH+Wings builds heavily on the design of DASH, and many features are inherent to both designs. The addition of wings and a larger control board containing an accelerometer on DASH+Wings lead to new issues that must be addressed to maintain the dynamic stability possessed by DASH. These issues necessitated the need for the design of a compliant foot to allow for proper tuning of the compliance in the system.

2.1 DASH - Dynamic Autonomous Sprawled Hexapod

There are several design features of DASH that directly impact using an accelerometer to measure the forces present on the robot. DASH takes advantage of a differential drive mechanism to transfer power from the motor to the legs. Due to the robot's lightweight construction, each end of the drive mechanism is a significant portion of the total mass. Because of this, DASH's center of mass does not correspond to a fixed point on the robot.

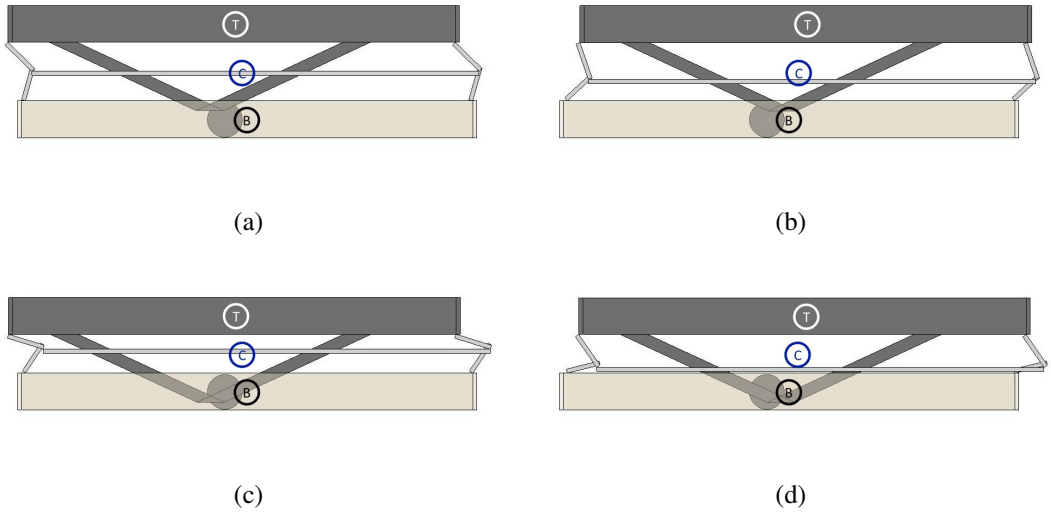

Figure 2.1: The top and bottom plate of DASH and DASH+Wings move based on the position of the motor to drive the output of the legs. Because each plate is a significant portion of the mass of the robot, the location of the center of mass is a weighted average of the position of the two plates and moves with respect to each plate as the robot runs. The center of each plate is marked, and the center of mass for the whole system is marked assuming each plate has equal mass.

Figure 2.1 shows the motion of the two plates over a revolution of the output gear. The location of the center of mass is a weighted average of the position of the two plates. It is not possible to directly measure the forces on the center of mass with an accelerometer; the accelerometer must be mounted to a location that moves with respect to the center of mass.

One of the central elements in the design is the use of the scaled Smart Composite Manufacturing (SCM) process to build the structure of DASH. This process allows rigid cardboard linkages with polymer hinges to be cut from a single flat piece and then folded into a three dimensional structure. These cardboard linkages are rigid to forces directed along the face of the beam but compliant when forces are directed into the face of the beam. In addition, the polymer hinges also add compliance to the system. The construction

of DASH orients the beams such that the power transmission from the motor to the legs is maximized. While running, dynamic loading causes the kinematics of the system to vary from the prescribed positions. This makes accurately predicting the location of the center of mass with respect to a known location on the body uniquely difficult.

2.2 Hybrid Locomotion - DASH+Wings

To examine the effect of flapping wings on terrestrial locomotion, the design of DASH is modified to include a wing drive mechanism along with the leg drive, as seen in Figure 2.2(a). The wing design is taken from a toy ornithopter (Interactive Toy's VAMP), and consists of a stiff leading edge spar attached to a flexible polymer anchored to the body at the rear corner (Figure 2.2(b)). The pivot of the wings connects to the top plate of the robot and the drive point links to the lower plate. As the two plates move in a circle to drive the legs the vertical portion of their motion drives the wings; from the kinematics of the system, the wing is at the top of its stroke when the right tripod is mid-stance and at the bottom of the stroke when the left tripod is mid-stance. The actual position of the wings with respect to the legs changes when the robot is dynamically running due to the compliance present in the mechanism and the high inertia of the wing. High speed video shows that the extremes of the wing stroke correspond to the end of the stance phases instead of the middle of the stance. The wings are easily removable, allowing the same robot to be tested both with and without wings, minimizing differences in performance due to construction variability.

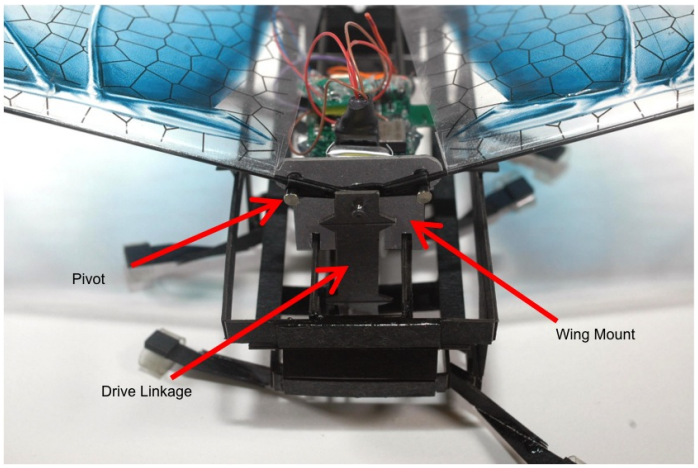

(a)

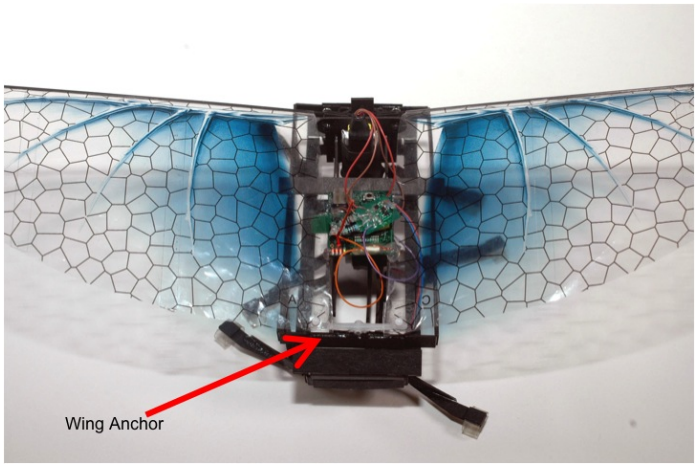

(b)

Figure 2.2: The wings are mounted to the top plate of DASH, with the drive linkage connected to the bottom plate, shown in (a). (b) shows the flexible wings anchored to the body at the rear corner of the wing.

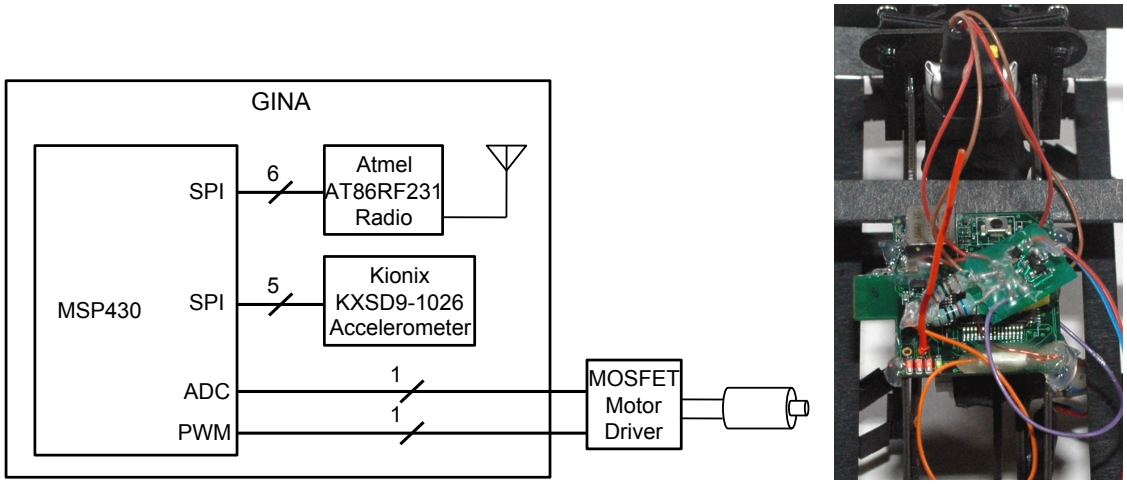

(a) (b)

Figure 2.3: DASH is fitted with a MSP430 processor, wireless radio, three axis accelerometer, and a small motor driver, outlined by (a). The whole package is 2.5 cm by 2.5 cm, and weighs 2.7 grams. The package is mounted on the top plate of the robot, shown in (b)

2.3 Accelerometer Integration

To measure the accelerations of the robot, DASH uses a custom PCB package known as GINA (General Inertial Navigation and Assistance) [9]. The electronics (Figure 2.3) include an MSP430 processor, interfaced with an Atmel AT86RF231 radio for wireless communication using the IEEE 802.15.4 protocol. The board also includes a Kionix KXSD9-1026, a tri-axis accelerometer with an adjustable sensitivity range and internal noise filter. The accelerometer is configured to measure ± 6 g's with the internal noise filter set to a cutoff frequency of 100 Hz. The processor interfaces with a small motor control board allowing the motor speed to be set with a PWM signal and the back EMF of the motor to be measured with an ADC channel. The MSP430 samples both the accelerometer and

motor back EMF signals at 500 Hz, and wirelessly transmits this information to a receiver. A Python script is used to interface with the receiver, check the validity of the packet, and store the data. In addition, the MSP430 runs a PID controller to regulate the motor velocity (detailed in section 2.4). Overall, the electronics package is 2.5 cm by 2.5 cm, and weighs 2.7 grams.

There are many advantages to using an accelerometer to measure the forces on the system over other methods. It allows the accelerations due to all of the forces to be measured simultaneously. A force plate is capable of measuring only the ground reaction forces, neglecting the aerodynamic forces of the wings. A VICON system can be used to accurately determine the position of the robot, but are expensive and not portable. MEMS accelerometers are very inexpensive, and can be used in any environment with the robot. Additionally, the integration of on board sensing can allow for future autonomous operation.

2.4 PID Motor Control

As DASH or DASH+Wings runs along the ground, the load on the motor varies by a large amount due to the stiffness of the structure, the foot contact, and the position of the wing stroke. With constant PWM control, this leads to a varying motor velocity throughout the course of a stride. This variation makes comparing multiple trials difficult, as the motor velocity profile of DASH and DASH+Wings are quite different, even with the same average motor frequency. To alleviate this problem, a Proportional-Integrative-Derivative controller

was implemented using the back EMF signal as motor feedback. The back EMF is sampled at 500 Hz; four samples are averaged to reduce noise and the controller is run at 125 Hz. The PWM value is calculated by:

$$PWM = K_p \times e[k] + K_d \times (e[k] - e[k-1]) + K_i \times \sum_{i=0}^{i \leq k} e[i]$$

The analog-to-digital converter gives a value for the back EMF signal ranging from 0-4095 which is subtracted from the desired value to compute $e[k]$. The output of the equation is a PWM value that ranges from 0-2000, with 2000 corresponding to 100% duty cycle. Anti-integral windup is also implemented, limiting the integration sum to ± 500 ADC counts. The PID gains were determined empirically by running the robot and looking at the variation of the back EMF signal. The values that resulted in the smallest variation were (in units of ADC counts per PWM value):

$$K_p = 15 \quad K_d = 1 \quad K_i = 2$$

2.5 Compliant Foot Design

An important feature in stable dynamic locomotion is the presence of compliance in the system. This can be seen throughout nature [10], as well as in many legged robots [1] [11]. Proper tuning of this compliance is necessary for good dynamic performance [12]. In the original version of DASH, the compliance was distributed throughout the structure, allowing for stable locomotion. In the modified version fitted for wings the overall structure is more rigid. The linkages used to mount and drive the wings function as cross bracing

on several of the beams in the structure, reducing their ability to flex under load. Adding the GINA mote also constrains the beams, further reducing the compliance present in the system. Finally, the GINA mote is a significant portion of the weight of the robot, and its addition raises the overall center of mass of the system. This further decreases the stability margin of the modified version of DASH, increasing the importance of proper tuning.

With the elimination of much of the compliance from the body of DASH, compliant feet are added to the legs to compensate and keep the relative stiffness optimal. There are several constraints that were kept in mind during the design of the feet. The first constraint is ease of integration with the cardboard manufacturing process. Any leg/foot design needs to be easily attachable to the rest of the structure. Secondly, the weight of the feet is very important. Because the feet are attached at the end of the legs and swing through the air rapidly, heavy feet greatly increase the inertia of the legs. This can cause problems in several areas, most notably with foot collisions at fast speeds. Finally, the feet should be easily tunable allowing the correct stiffness to be properly selected.

The foot design that met all of these criteria is a basic polymer loop added to the end of a rigid cardboard leg, shown in Figure 2.4. This is directly integrable with the cardboard process, and the addition of the polymer loop adds only 40 milligrams to the leg. There are several ways the legs can be appropriately tuned to the correct value. The thickness of the polymer film can be adjusted to coarsely tune the stiffness. The length and width of the loop can then be adjusted to more finely select the correct stiffness. A measurement of the stiffness can be determined by using the accelerometer to measure the resonant frequency

(a) (b) (c)

Figure 2.4: A polymer loop on the end of a rigid leg adds compliance to the robot (b). The leg easily integrages with the folded cardboard process (a) used to build the rest of the structure. The accelerometer is used to measure the resonant frequency of a tripod with the polymer loop legs attached, as well as the legs with the polymer loop removed. (c) shows the accelerometer data from this measurement. The polymer loop legs give the tripod a resonant frequency of 7.7 Hz, while the resonant frequency of the tripod with cardboard legs is 10.7 Hz.

of the system. As seen in Figure 2.4, the resonant frequency of a tripod is 7.7 Hz for the polymer loop legs and 10.7 Hz for the cardboard legs. The polymer loop legs have a tripod stiffness of 50.1 N/m in the normal direction, corresponding to a vertical stiffness of 16.7 N/m per leg. The compliant legs were chosen to reduce amplitude of oscillation in the normal direction at higher running speeds, improving the stability of the robot. This leads to a resonant frequency lower than the desired running frequency.

Chapter 3

Methods

When the robot is smoothly running along level ground at a constant average velocity, the average acceleration in both the normal and fore-aft directions is zero, and does not convey any information about the forces acting on the system. To understand the effects of wings on a running robot, it is necessary to examine the variations in acceleration during the course of a single stride. As the robot runs, the accelerations measured by the IMU can be thought of as a periodic signal with some noise. There are two main periodic components to the acceleration signal, the motor crank frequency, and the stride frequency at twice that of the motor (unless the stride frequency is explicitly specified, the motor crank frequency is referred to as the frequency of the system throughout this paper). When wings are added to the robot, the accelerometer also measures both the aerodynamic and inertial forces due to the wings. These forces are also periodic at the same frequency as the motor frequency. The noise in the system comes from two main sources. The first is simple measurement noise

from the accelerometer. The second comes from variations in the foot-ground interaction. For this reason, many strides should be compared to get an accurate description of the forces on the robot during a stride.

3.1 Data Conditioning

Because of the use of wireless data collection, data packets can be dropped or corrupted leading to unevenly spaced data points. In a typical trial, around 5% of packets will be lost. The missing data points are replaced by linearly interpolating from the surrounding values. This gives a data set with a constant sampling frequency, allowing the use of digital filters. To reduce the noise present in both the accelerometer and back EMF signal, a third order Butterworth filter with a cutoff frequency of 100Hz is applied to the signals. The data are run though the filter both forwards and backwards resulting in zero phase distortion. This also has the effect of squaring the magnitude response and doubling the order of the filter, giving an effective sixth order filter.

When comparing different strides, the data need to be resampled to allow a point to point comparison between strides. This is especially relevant when phase is used to parametrize the measurements. In this case each sample is not evenly spaced, and the data points for each stride do not line up evenly. To resample the data, a cubic spline is fit to the dataset, and samples are taken at even intervals. Figure 3.1 shows a series of data points, with the cubic spline fit. The original data is sampled at a high enough rate that resampling

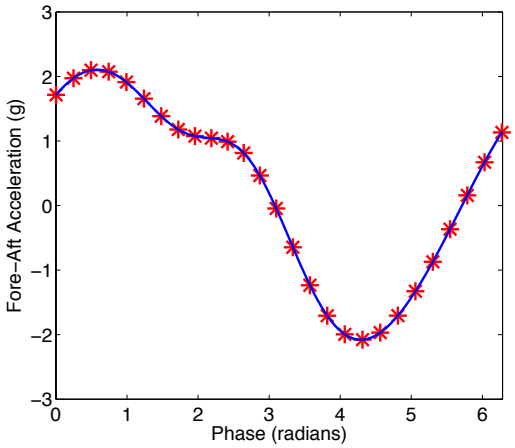

Figure 3.1: Accelerations from a sample motor cycle. The original data points are shown, overlaid by a cubic spline approximation. The cubic spline is used to resample the data at even crank phase intervals.

is possible, and the strides can be analyzed and compared to each other.

3.2 Open Loop Synchronization

When the robot is run at a constant PWM, or open loop, the back EMF signal shows a large periodic variation in the motor velocity from the structural stiffness present in the robot. The velocity varies with the phase of the output gear of the motor (simply referred to as motor phase from now on), and the back EMF signal is used to synchronize multiple motor cycles. Each cycle of the motor is equivalent to two strides, or one stride per tripod. By selecting the peaks of the back EMF signal as seen in figure Figure 3.2(a), the accelerations can be synchronized. Because of slight variations in the period of each cycle, the signals have low variability at the start and vary more near the end of the cycle

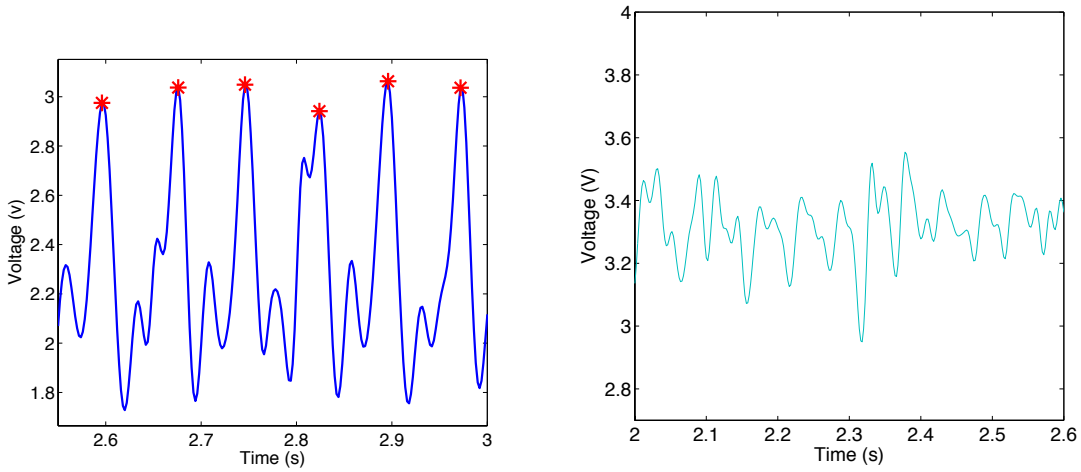

(a) Fixed PWM duty cycle

(b) PID velocity control

Figure 3.2: The back EMF signal when the robot is running with fixed PWM duty cycle (open loop velocity control) (a) and closed loop velocity control (b). The open loop signal has a larger peak to peak variation, and can more easily be used for stride detection.

(Figure 3.3(a)). Figure 3.3(b) shows the cycles scaled so they all have the same period, reducing the deviation in the acceleration signal from stride to stride.

Motor phase can also be used to parameterize the acceleration data and sync the cycles. By integrating the back EMF data and multiplying by a scale factor, the phase of the motor can be determined. This scale factor is proportional to the back EMF constant of the motor times the gear ratio, but varies slightly due to variations in battery voltage, filtering of the back EMF signal, and individual variations between motors. However, the scale factor can be determined from the back EMF signal itself, because one cycle of the motor is evident from the change in velocity. The factor can be determined on a per cycle basis, by integrating the back EMF and multiplying by the scale factor necessary for the phase

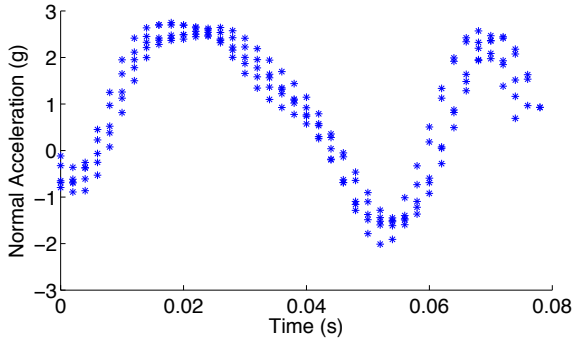

(a) Acceleration vs. original sampled time

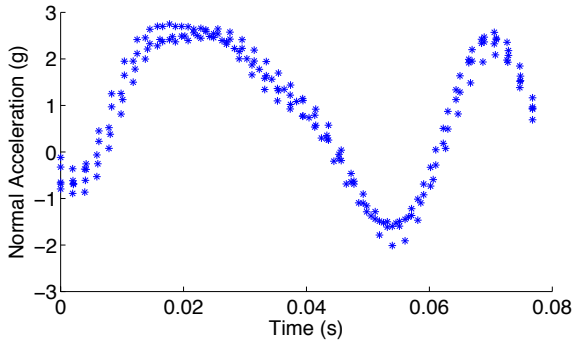

(b) Acceleration vs. scaled time

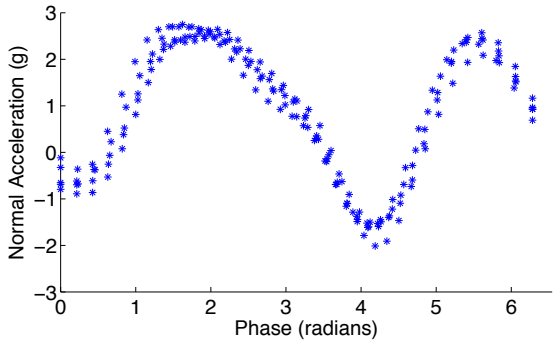

(c) Acceleration vs. scaled phase

Figure 3.3: A comparison of the different ways the data can be parameterized by using the back EMF data to separate the data into cycle intervals. (a) shows the data vs. the original sample time, while in (b) each interval has been scaled to an equal period. In (c), the signal is parameterized using the phase of the motor computed from the back EMF signal.

to integrate to 2π over the cycle. Using this method, the scale factor ranges from 0.0331 rad/s/ADC count to 0.0390 rad/s/ADC count for the different intervals over the course of a run. The variations over in this factor are caused by slight changes in the peak to peak spacing. Figure 3.3(c) shows the results of this method, which results in good correlation between strides.

3.3 Closed Loop Synchronization

When a PID controller is applied to the motor, the back EMF signal is regulated to a set point and distinct cyclic variations can no longer be seen (Figure 3.2(b)). However, there is still a strong periodic component to the acceleration signal itself. To partition the data into intervals in this case, the data are first parameterized using the integral of the back EMF. They are then multiplied by a base scale factor (chosen based on experience from the open loop case). The data are split into cycles by taking the phase modulus 2π and the cycles are compared by computing the correlation coefficient between each cycle. The back EMF scale factor is then varied about the initial value chosen, and the correlation coefficient matrix is maximized. Unlike the open loop case only a single scale factor is used, instead of an individual factor per cycle. This fits better with the physics of the system – since the battery voltage is approximately constant during a single run, the motor should have a single scale factor proportional to the back EMF constant. A typical value for the back EMF scale factor is 0.0347 rad/s/ADC count, with a variation of less than 10% run to

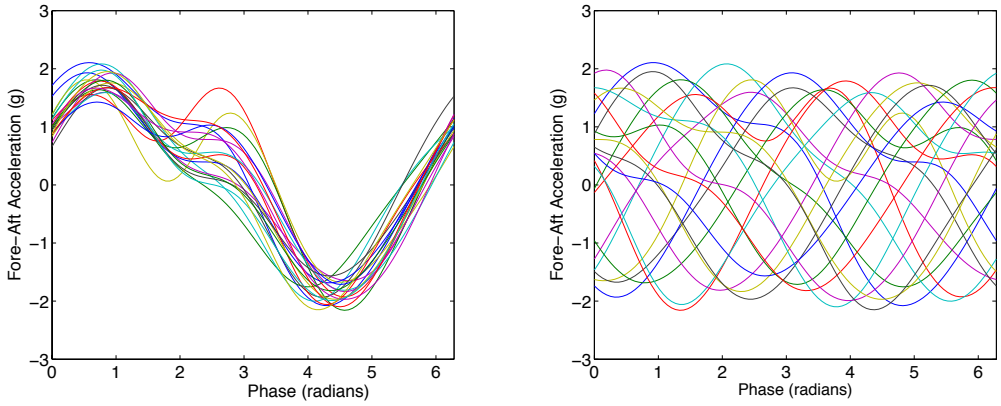

(a) Individual strides with correct scale factor (b) Individual strides with scale factor off by 5%

Figure 3.4: To determine the back EMF scale factor without a strongly periodic back EMF signal to use for dividing the intervals, the correlation in the acceleration between successive cycles is used. The back EMF scale factor is selected to maximize the correlation between the cycles, shown in (a). This scale factor can change slightly from trial to trial due to factors such as the battery voltage. A variance of only 5% in the scale factor causes the cycles to be very poorly synchronized, as shown in (b), precluding the use of a constant scale factor for every trial.

run. Choosing the correct value is imperative, as Figure 3.4 shows; an error of just 5% in the scale factor gives very poor synchronization. The high degree of periodicity in the acceleration measurements due to the differential motion of the plates and the stride forces can be used to accurately synchronize the datasets to the motor phase, without explicitly measuring the phase of the motor.

Chapter 4

Results

To examine the effect of wings on terrestrial locomotion, running on both level and inclined surfaces are examined. By running up a sloped surface, the maximum average thrust of the robot is determined, without the effects of drag. On a level surface, an accelerometer is added to the robot to measure the varying forces present on the robot during the course of a stride. By exploring these two methods, the difference in locomotion between a legged robot both with and without wings are quantitatively compared. The acceleration data are also used to examine different gaits that arise when the legs are not properly tuned.

4.1 Incline running

To examine the abilities of DASH and DASH+Wings to run up an incline, a tail was added to stabilize the ascent, and prevent the robot from turning and running down the slope. The robots were then run up an incline, and the slope was increased until the robot

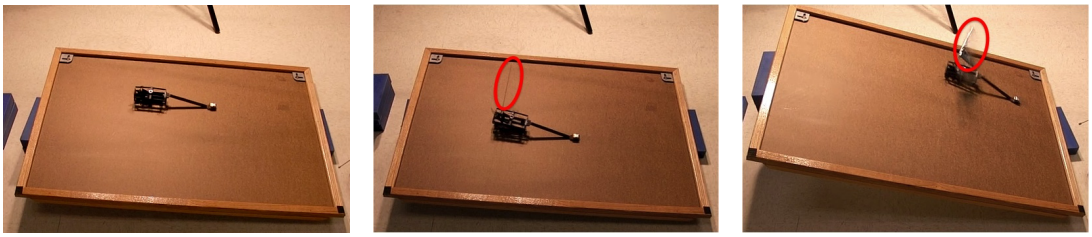

(a) DASH (b) DASH+Inertial Spars (c) DASH+Wings

Figure 4.1: The robot running up a slope, with legs only (a), legs plus inertial spars (b), and legs plus wings (c). The right inertial spar in (b) and the right wing in (c) are circled in the photographs above. DASH+Wings is capable of climbing significantly higher slopes than either of the other variants.

Table 4.1: Inclined Running Results

Configuration	DASH	DASH+IS	DASH+Wings
Maximum Slope (% Grade)	8.9	8.9	32.9
Avg. Thrust Generated (mN)	29	29	104

could no longer make forward progress on the slope. The thrust was computed from the force needed for the robot to propel its own weight upward at that slope against gravity. The basic cardboard feet that are used have a static friction coefficient of 0.34 and a kinetic friction coefficient of 0.31 on the inclined surface. From this measurement, the maximum slope the robot would be expected to traverse using static friction alone is 18.8 degrees, or a 34% grade. When actually traversing the slope the forces are limited by the kinetic friction, which limits the maximum slope to a 31% grade (17.2 degrees). As a control, inertial spars were also added to the robot to determine if the inertial or aerodynamic forces from the wings had the greater effect.

Table 4.1 summarizes the results of the inclined running. The amount of force produced by the robot is computed from the force needed to propel the weight of the robot up the slope against gravity. The addition of wings to DASH allows the robot to climb slopes 3.7 times greater and produce 75 mN more thrust than the robot with legs alone. DASH+Wings is actually able to dynamically climb slopes that are outside of the friction cone of the surface. The addition of inertial spars to DASH has no effect on the inclined running, demonstrating that it is the aerodynamic properties of the wings that enable the increase in abilities.

4.2 Level Running

Adding an accelerometer to DASH and DASH+Wings allows the comparison of the instantaneous forces generated on the robot during level running. The accelerometer data can be synchronized with high speed video, and the forces caused by specific events such as a foot hitting the ground or a downbeat of the wing can be determined. The high speed video was also used to filter out startup transients and determine when the robot reached constant forward velocity. By integrating the accelerations, the trajectory of the robot can be determined during a single cycle. The accelerations and trajectories of DASH and DASH+Wings at similar frequencies, as well as at maximum speed can be compared.

The differential motion of the drive plates detailed in section 2.1 has a significant effect on the acceleration signal. The accelerometer is mounted on the top plate, which moves

relative to the center of mass as the two plates move throughout a revolution of the motor. This motion can be clearly seen by comparing position of the marker on the top plate relative to the marker for the center of mass in Figure 2.1. The effect of this motion on the acceleration signal can be examined by looking at the data while the robot is in free-fall (Figure 4.2). In free-fall, the only acceleration experienced by the center of mass is from the force due to gravity. The signal measured by the accelerometer (mounted on the top plate) is due only to the motion of the accelerometer with respect to the center of mass. The distribution of the mass between the two plates determines the magnitude of the relative motion of the plate and the center of mass. The acceleration signal is also affected by the speed at which the motor moves the plates. When running along the ground, the accelerometer measures the forces on the center of mass from the foot ground interaction and aerodynamics of the wings superimposed with the motion of the accelerometer with respect to center of mass.

Figure 4.3 shows the acceleration loop for several motor cycles of DASH with the footfall events superimposed on the graph. Likewise, Figure 4.4 shows several cycles of DASH+Wings with the footfall and wingbeat events shown. When running smoothly, the accelerations experienced by the robot during the course of a cycle are very periodic and repeatable. Additionally, the stride events happen at a predictable and repeatable phase. By averaging multiple cycles of data, the accelerations experienced over a typical cycle can be compared for DASH and DASH+Wings. Figure 4.5 also shows the accelerations experienced by the robot in free-fall. The robot exhibits a distinctly different pattern of

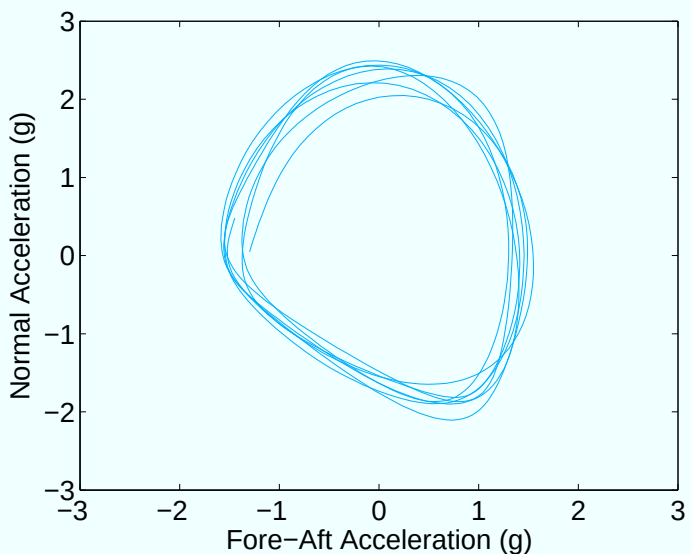

(a) Normal Acceleration vs. Fore-Aft Acceleration

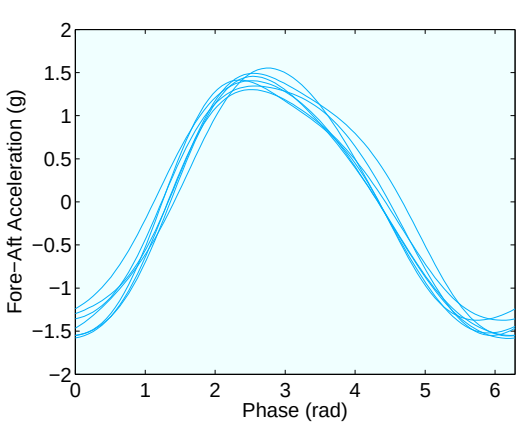

(b) Fore-Aft Acceleration vs. Phase

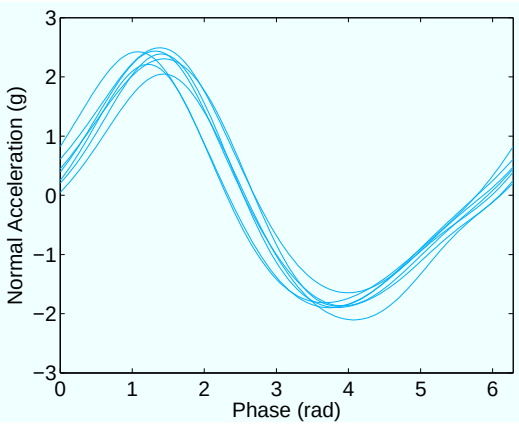

(c) Normal Acceleration vs. Phase

Figure 4.2: Measured Accelerations in free-fall at 19.5 Hz. Seven motor cycles are shown, parameterized by phase. (a) shows the normal acceleration plotted vs. the fore-aft acceleration, while (b) and (c) show the accelerations plotted vs. motor phase. While center of mass is only affected by gravity in free-fall, the top plate shows a large acceleration signal caused by the relative motion of the mounting point of the accelerometer on the top plate and the center of mass. This relative motion can be seen by looking at the markers for the center of mass and the top plate in Figure 2.1.

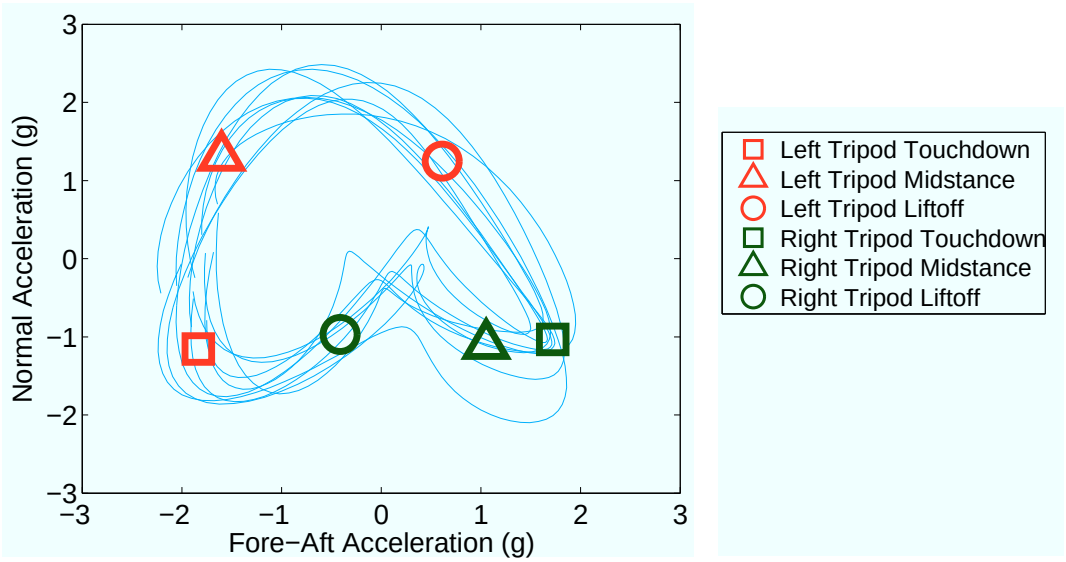

(a) Normal Acceleration vs. Fore-Aft Acceleration

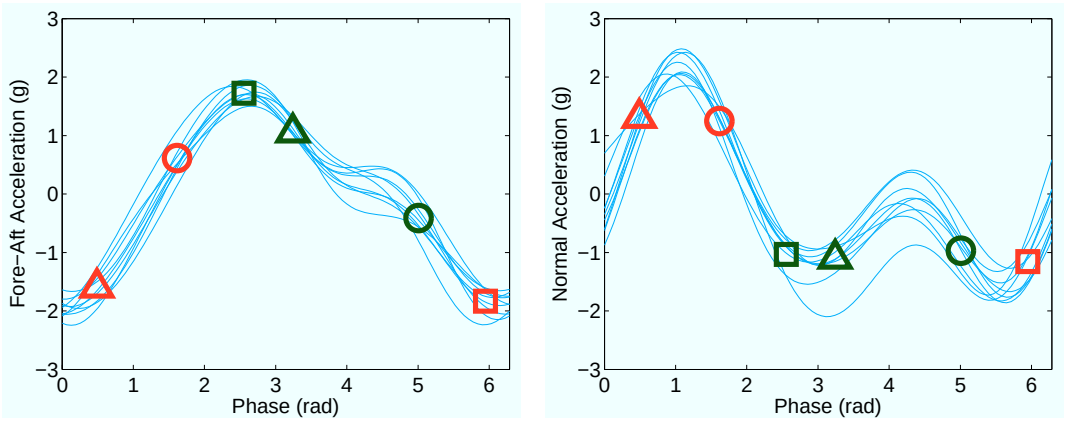

(b) Fore-Aft Acceleration vs. Phase

(c) Normal Acceleration vs. Phase

Figure 4.3: Measured Accelerations for DASH running at 19 Hz. Nine motor cycles are shown, parameterized by phase. (a) shows the normal acceleration plotted vs. the fore-aft acceleration, while (b) and (c) show the accelerations plotted vs. motor phase. High speed video was used to determine the location of stride events within each cycle. One complete cycle, or revolution, of the motor corresponds to 2 strides.

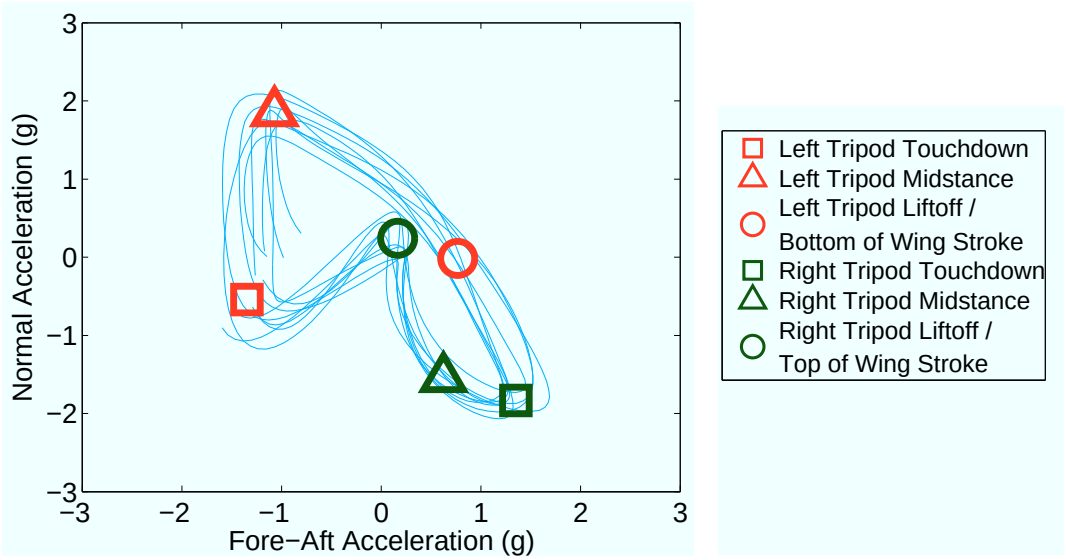

(a) Normal Acceleration vs. Fore-Aft Acceleration

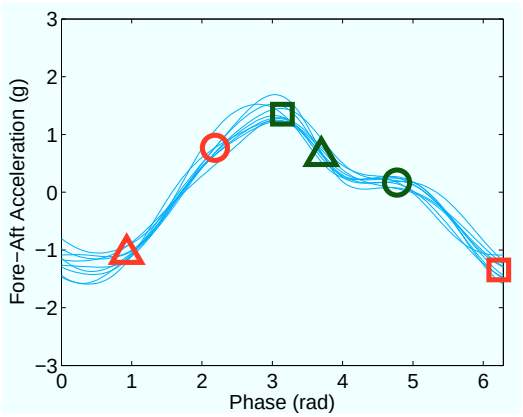

(b) Fore-Aft Acceleration vs. Phase

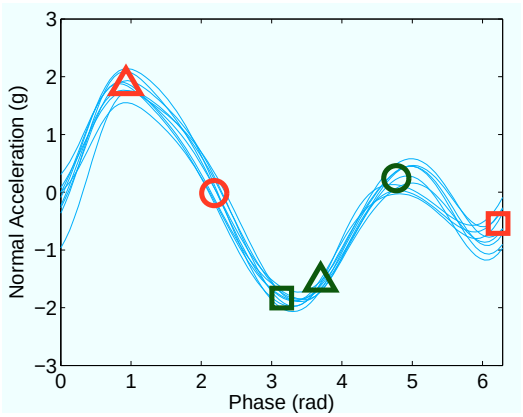

(c) Normal Acceleration vs. Phase

Figure 4.4: Measured Accelerations for DASH+Wings running at 14.2 Hz. Nine motor cycles are shown, parameterized by phase. (a) shows the normal acceleration plotted vs. the fore-aft acceleration, while (b) and (c) show the accelerations plotted vs. motor phase. High speed video was used to determine the location of stride events within each cycle. One complete cycle, or revolution, of the motor corresponds to 2 strides.

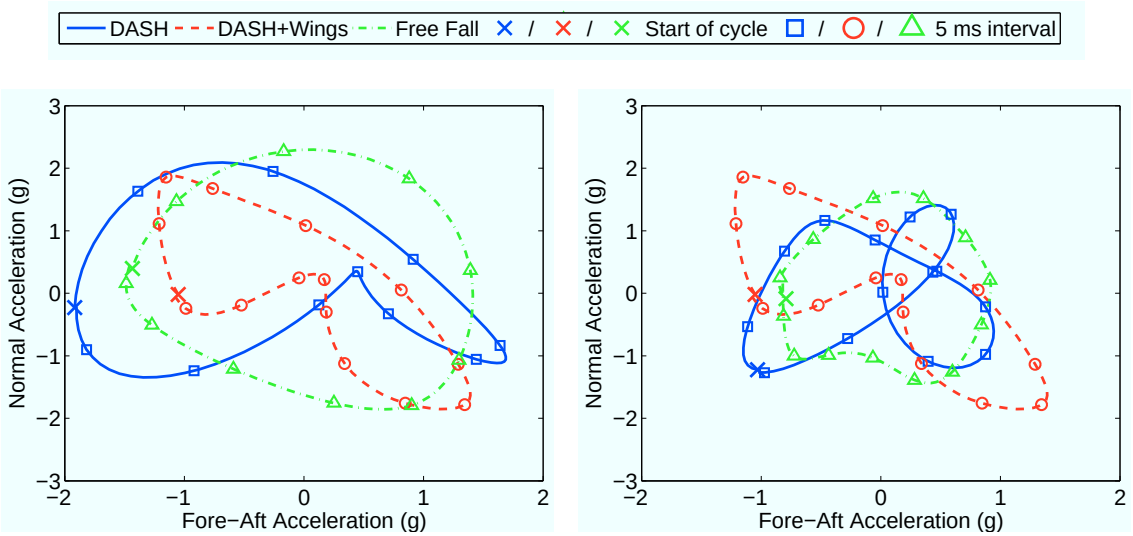

(a) Maximum speed

(b) Matched Frequency

Figure 4.5: Measured Acceleration Loop for DASH and DASH+Wings running at their maximum speed (a) and at the same frequency (b). In (a), DASH is running at 19 Hz, while DASH+Wings is running at 14.2 Hz. In (b), both are running at 14.2 Hz. The acceleration measured in free-fall for motor frequencies of 19.5 Hz in (a) and 14.2 Hz in (b) is included for comparison in each plot.

accelerations in the three different cases: differential plate motion only, differential plate motion plus ground contact forces, and differential plate motion plus ground contact forces and wing forces (both aerodynamic and inertial).

Figure 4.5(a) shows the acceleration loops when DASH and DASH+Wings are running at their maximum speeds. For DASH, this is 1.45 m/s at a motor frequency of 19 Hz. DASH+Wings is running at 1.34 m/s with a motor frequency of 14.2 Hz. The slower motor frequency of DASH+Wings is due to the higher load on the motor from the wings, and the maximum amount of power the battery can provide. By running DASH at the slower frequency that DASH+Wings runs at, the accelerations can also be compared between the two

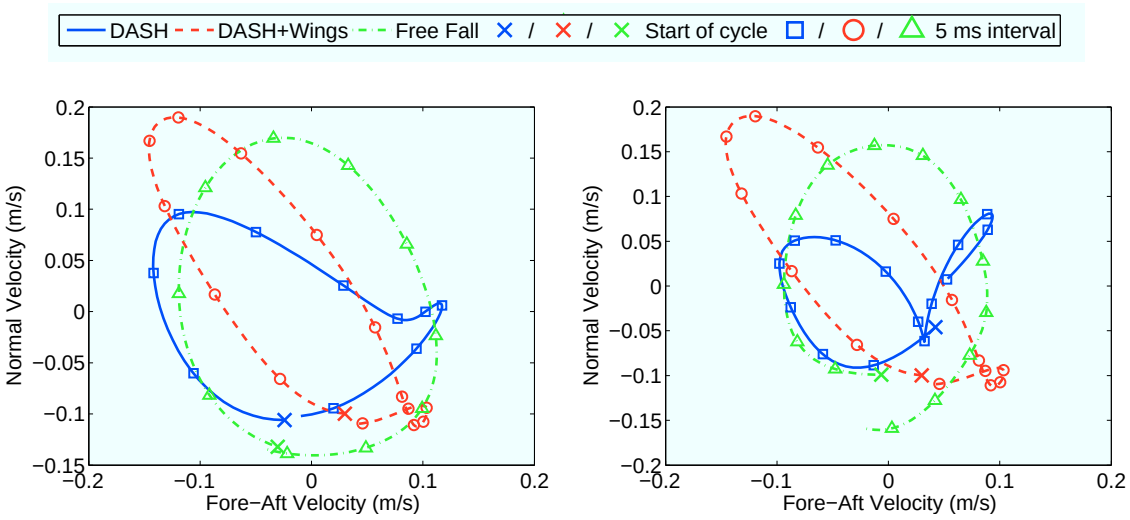

(a) Maximum speed

(b) Matched Frequency

Figure 4.6: Velocity Loop DASH and DASH+Wings running at their maximum speed (a) and at the same frequency (b), determined by integrating the acceleration over an average cycle. In (a), DASH is running at 19 Hz, while DASH+Wings is running at 14.2 Hz. In (b), both are running at 14.2 Hz. The average horizontal velocity is normalized to zero to allow the loops to be overlaid for comparison. The velocity measured in free-fall for motor frequencies of 19.5 Hz in (a) and 14.2 Hz in (b) is included for comparison in each plot.

robots running at the same stride frequency. Figure 4.5(b) shows the different forces that are produced when DASH is run at a slower frequency to match that of DASH+Wings. The difference in trajectories is more pronounced at matched frequencies than in the maximum speed case.

By integrating the accelerometer data, the velocity and position of the robot during a cycle can be determined. Figure 4.6(a) and Figure 4.6(b) show the difference in the instantaneous velocity over the course of a cycle between the different configurations, again at both maximum speed and matched frequency. By looking at the position of the robot in Figure 4.7, the different trajectories taken by the robot over the course of a cycle can be

seen. DASH+Wings has a much larger vertical oscillation over the course of a cycle than DASH. When run at maximum speed, the velocity of DASH and DASH+Wings is very similar, while at equal motor frequencies DASH+Wings covers much more ground.

4.3 Hop Gait

The addition of an accelerometer to DASH also allows the study of non-smooth gaits. Figure 4.8 shows DASH running with poorly tuned legs. This causes the robot to hop in the air, and several strides to miss contact with the ground completely. This behavior leads to high vertical oscillations and poor horizontal locomotion. Due to the hopping behavior, the accelerometer data shows a period of two motor cycles, rather than the one cycle period seen in a smooth gait. Figure 4.9 shows the data synchronized with a one cycle and a two cycle period. The average correlation coefficient between cycles is 0.47 for a one cycle period, and 0.63 for the two cycle case. Although a better correlation coefficient is seen in the two cycle case, it is still much lower than the 0.9 or higher seen when the robot is properly tuned.

Figure 4.10 shows the motion of the robot during the hopping gait compared to the smooth trajectory. It is immediately apparent in Figure 4.10(a) that the majority of the force is directed in the normal direction, instead of the horizontal direction where it can contribute to the forward locomotion of the robot. This leads to much larger vertical velocities over the course of a period (Figure 4.10(b)), and consequently larger vertical displacement while

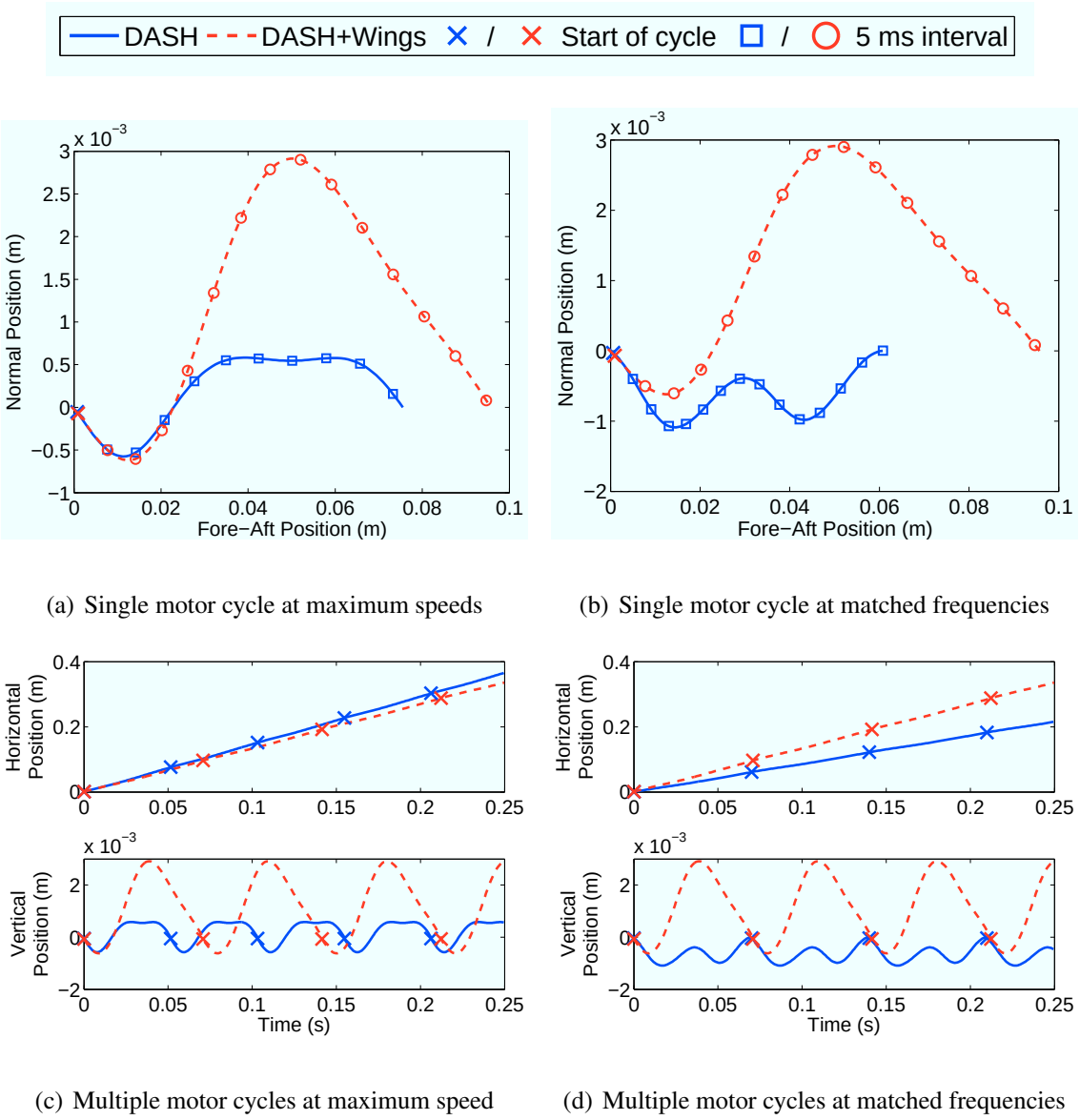

(a) Single motor cycle at maximum speeds

(b) Single motor cycle at matched frequencies

(c) Multiple motor cycles at maximum speed

(d) Multiple motor cycles at matched frequencies

Figure 4.7: Vertical and Horizontal position for DASH and DASH+Wings. (a) and (b) show a single motor cycle, while (c) and (d) show several average motor cycles strung together. A comparison is shown for DASH and DASH+Wings running at their maximum speed (a, c), determined from high speed video to be 1.45 m/s and 1.34 m/s respectively. The comparison is also shown for the case of equal motor frequencies (b, d), with DASH running at 0.86 m/s, and DASH+Wings running at 1.34 m/s. The top plots show the trajectory of the top plate over a single cycle, and the bottom plots show the position of the top plate vs. time over several average cycles.

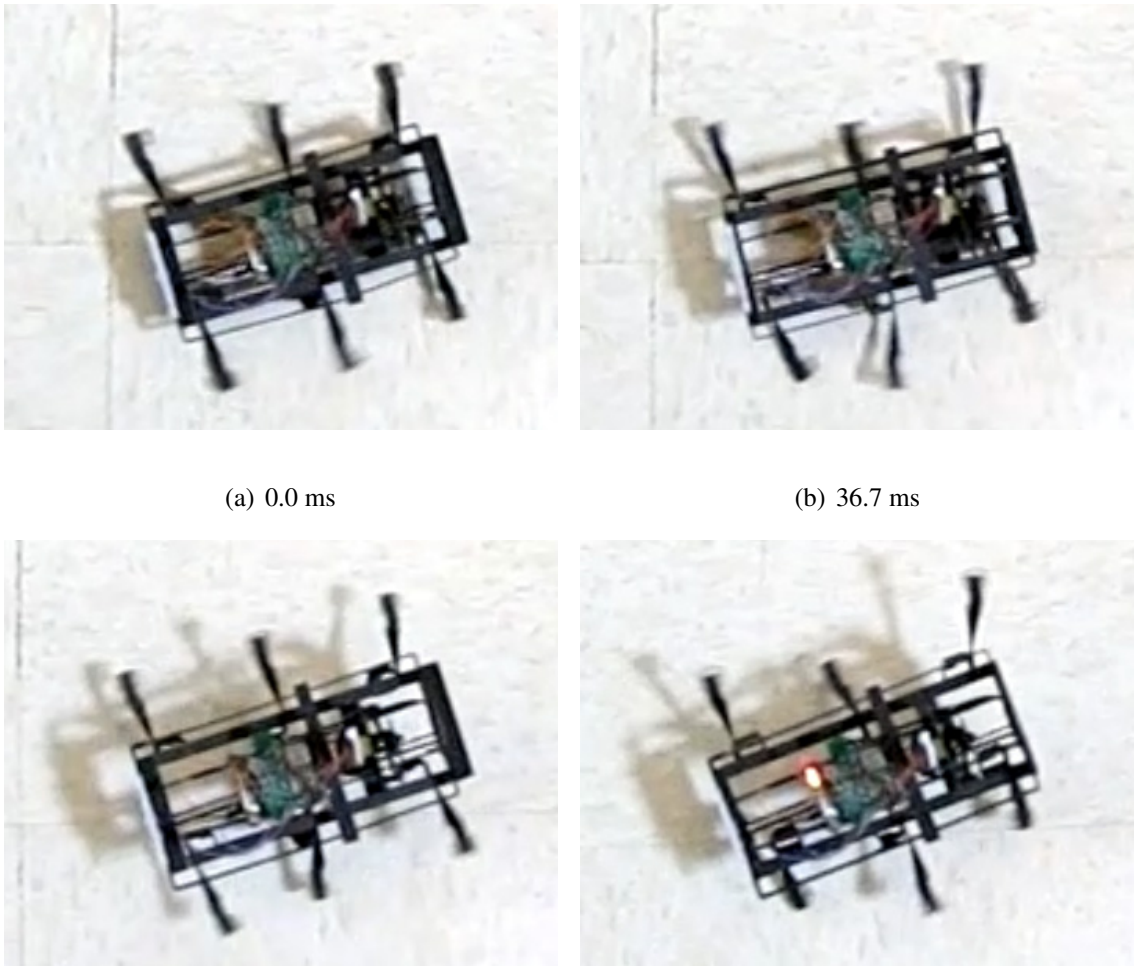

(a) 0.0 ms

(b) 36.7 ms

(c) 86.7 ms

(d) 91.0 ms

Figure 4.8: DASH running with a hop gait. Figs. (a) and (b) show successive tripods in stance phase with the feet in contact with the ground. On the next cycle the robot is propelled upwards and the tripods are not touching the ground during the typical mid-stance portion of each stride in Figs. (c) and (d)

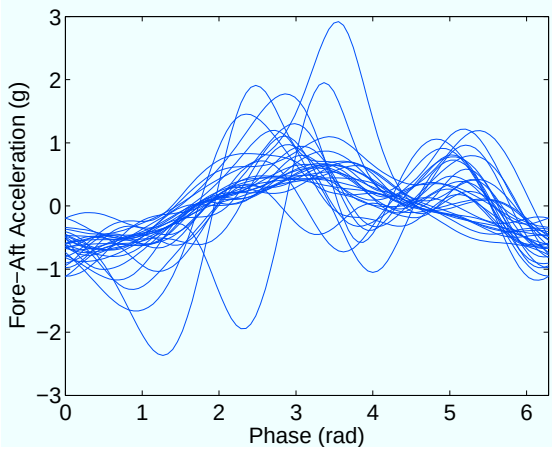

(a) Fore-Aft acceleration correlated over a single cycle

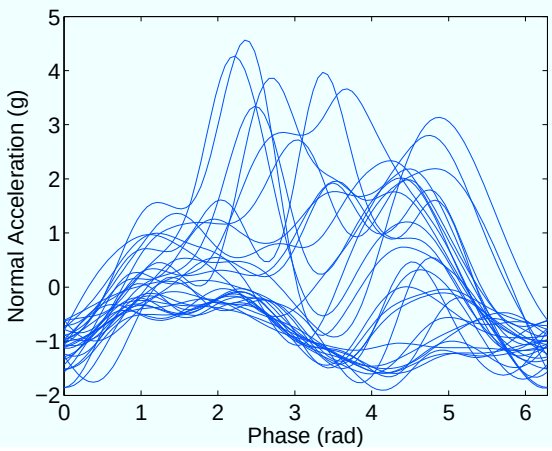

(b) Normal acceleration correlated over a single cycle

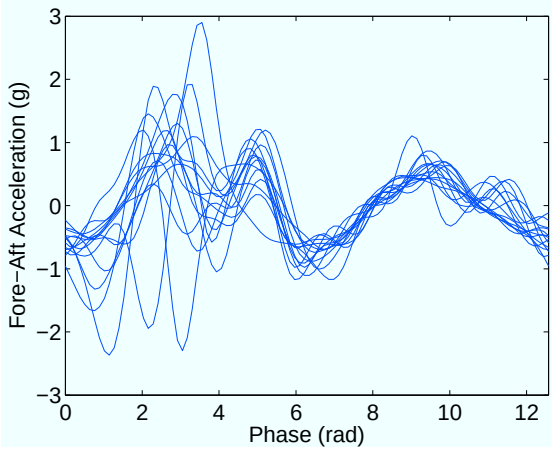

(c) Fore-Aft acceleration correlated over two cycles

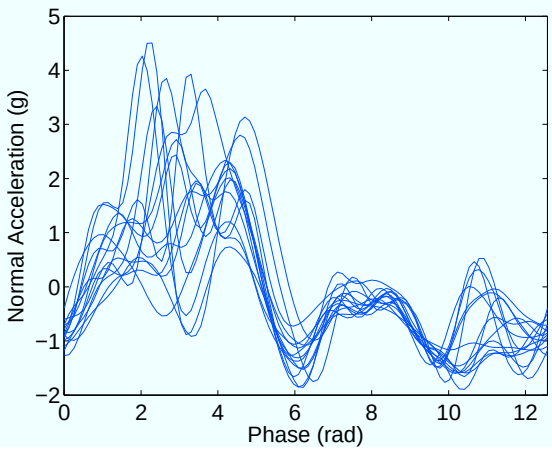

(d) Normal acceleration correlated over two cycles

Figure 4.9: Normal and Fore-Aft acceleration pattern of a hopping gait, based on a one cycle (a, b) and two cycle (c, d) period. When correlated over a single cycle, the average correlation coefficient between cycles is only 0.47. Over a two cycle period the correlation coefficient is 0.63, showing the effects of the hopping gait on the locomotion period.

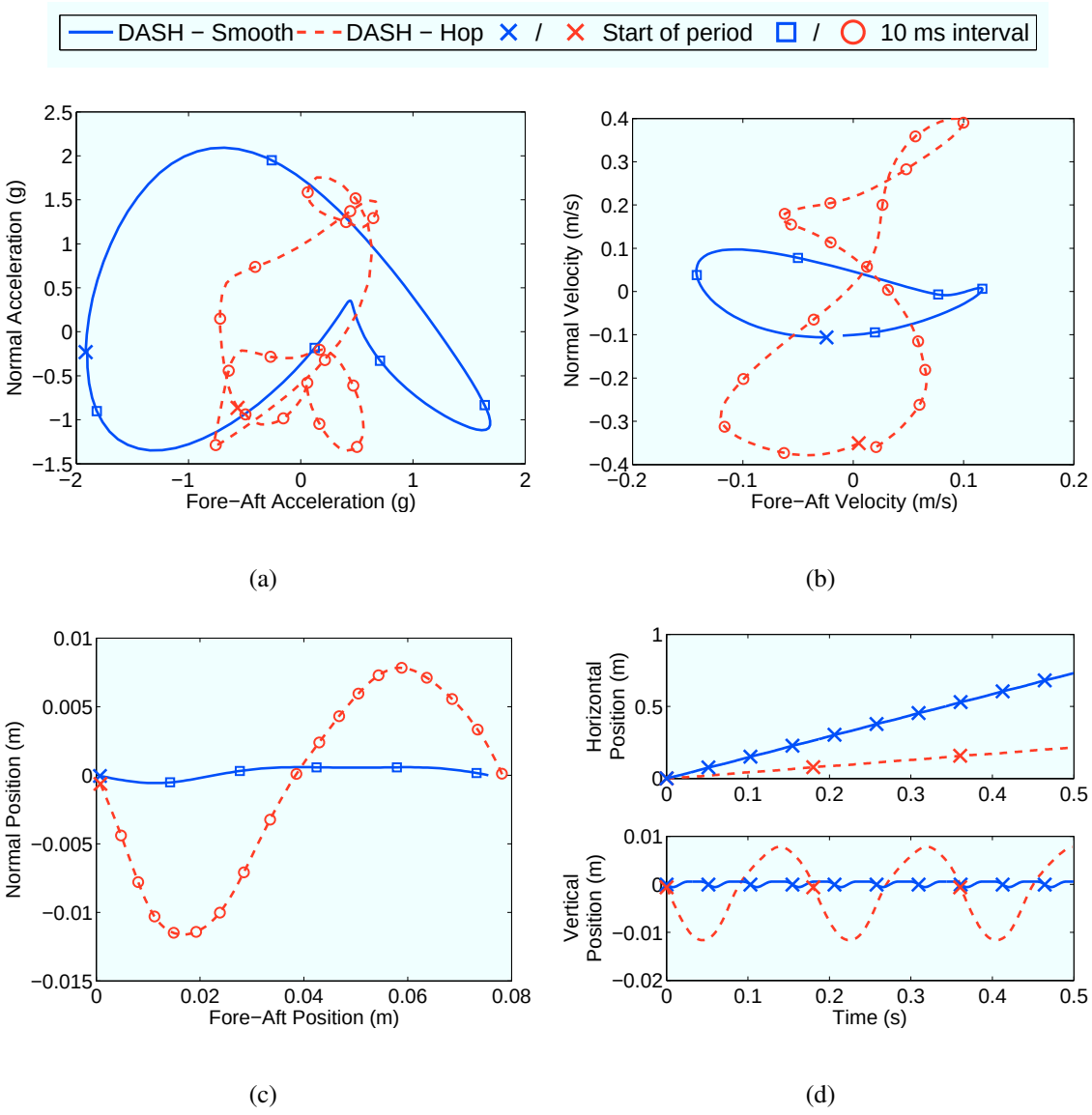

Figure 4.10: The hopping gait exhibited by the robot when poorly tuned shows a significantly different pattern of acceleration during a period (a). Most of the force is directed in the normal direction, and does not do useful work propelling the robot forward. (b) shows the velocity over the course of a period, with the average horizontal velocity normalized to zero for comparison. (c) shows the trajectory of the top plate over a single average period, while (d) shows the position of the top plate vs. time over several average periods.

running. Figure 4.10(c) shows the the vertical displacement of the hopping gait to be 20 mm, over 16 times greater than the 1.2 mm displacement when running with a smooth gait. The total distance traveled over a period in each gait is nearly equivalent, but the period of the hopping gait is much longer than that of the smooth gait. With a smooth gait, DASH travels 3.4 times faster than in an untuned system, shown by Figure 4.10(d).

Chapter 5

Discussion and Conclusions

The addition of wings to DASH gives a clear advantage in inclined running, with DASH+Wings able to traverse slopes much steeper than those DASH is capable of climbing. DASH+Wings is even capable of climbing inclines greater than the friction cone of the surface. This added mobility can enable access to a variety of natural environments previously inaccessible to the robot. The added thrust does require additional power, with the overall stride frequency reduced by the addition of wings. On level ground, the higher stride frequency of DASH allows it to maintain a higher overall velocity than DASH+Wings. When running at the same frequency however, DASH+Wings far outpaces its unwinged counterpart.

The accelerometer has proved a useful tool for measuring the accelerations seen by DASH and DASH+Wings while running. The accelerations experienced by DASH+Wings are clearly unique from those seen by DASH, at both maximum speed and matched fre-

quencies. The effect of these differences in acceleration can be seen by twice integrating the signal and observing the trajectory of the robot. The downstroke of the wing during the first portion of the motor cycle causes DASH+Wings to begin moving on an upward trajectory, reaching a peak height greater than that of DASH. This higher vertical trajectory combined with the high thrust produced by the wings may help DASH+Wings surmount obstacles in its path. The negative vertical acceleration due to the upstroke of the wing causes a downward motion in the trajectory of the robot.

By studying the fore-aft accelerations, the overall running speed of the robot can be determined. When running at a constant velocity, the negative accelerations due to losses in the system from forces such as friction evenly balance the positive accelerations from the legs and wings. By increasing the maximum acceleration produced by the robot, a greater velocity can be achieved before the losses are able to account for these forces and cause the robot to settle at a constant velocity – indeed a strong correlation can be seen between the maximum fore-aft acceleration experienced by the robot and the maximum velocity. At 19 Hz, DASH has a slightly higher maximum fore-aft acceleration than DASH+Wings and is also slightly faster. When running at 14.2 Hz, DASH has a significantly lower fore-aft accelerations, and is correspondingly slower than the winged DASH.

The addition of wings to DASH appears to increase the overall stability of the system, and decrease the importance of leg tuning. Because of the high center of gravity on DASH from the addition of the GINA mote, proper leg tuning is very important in maintaining the stability of the system. Perturbations to the system often cause uncontrollable oscillations

about the roll axis of the robot, generally terminating with the robot flipping over. With the addition of wings, DASH+Wings is tolerant of many different leg designs and rarely experiences any unstable oscillations.

The accelerometer has proved useful for identifying smooth running motions, as well as alternate hop gaits caused by improper tuning. During a smooth running gait the correlation between successive motor cycles is very high. When the robot is not running smoothly a much lower correlation between cycles is seen, and the robot can also have multiple cycle periods. The correlation between motor cycles can be used as a quantitative measure of the running performance. When the robot is not running smoothly, there tends to be more variability and randomness in the acceleration data leading to poor correlation. By tuning the robot to maximize the correlation between the acceleration signal over successive cycles, smooth running performance can be achieved.

Future work on DASH+Wings consists of using accelerometer data to improve the overall design, thereby increasing the mobility of DASH+Wings through the generation of higher thrust. By increasing the generated thrust, the robot should be able to climb steeper inclines, as well as achieve higher horizontal velocities. The current accelerometer data shows the accelerations of the top plate of DASH and DASH+Wings. The data includes the motion of the top plate with respect to the center of mass. Using the kinematics of DASH along with knowledge of the motor phase, the measured accelerations can be transferred to the center of mass of the robot. By studying the accelerations of the center of mass, a comparison can be made with previous models of dynamic locomotion, such as

the spring-loaded inverted pendulum model [10] and the lateral leg spring model [13]. The accelerometer data is also useful for studying different patterns of locomotion on DASH, and can be used as an additional quantitative measure of running performance.

Acknowledgments

The author would like to thank Ron Fearing for all of his assistance and guidance on this work, and Robert Full for the many discussions and suggestions for improving the results. Great thanks to Paul Birkmeyer for the use of DASH as a starting platform for this research, as well as the many design discussions and ideas generated, and to Ankur Mehta, for the use of the GINA mote. Finally, thank you to all of my colleagues in the Biomimetics Millisystems Lab for all of your comments and suggestions throughout the course of the work.

Bibliography

[1] U. Saranli, M. Buehler, and D. Koditschek, "Rhex: A simple and highly mobile hexapod robot," *The International Journal of Robotics Research*, vol. 20, no. 7, p. 616, 2001.

[2] J. H. Park and K.-J. Yoon, "Designing a biomimetic ornithopter capable of sustained and controlled flight," *Journal of Bionic Engineering*, vol. 5, no. 1, pp. 39 – 47, 2008.

[3] M. Bundle and K. Dial, "Mechanics of wing-assisted incline running (WAIR)," *Journal of Experimental Biology*, vol. 206, no. 24, p. 4553, 2003.

[4] K. Dial, "Wing-assisted incline running and the evolution of flight," *Science*, vol. 299, no. 5605, p. 402, 2003.

[5] P. Burgers and L. Chiappe, "The wing of Archaeopteryx as a primary thrust generator," *Nature*, vol. 399, no. 6731, pp. 60–61, 1999.

[6] P. Birkmeyer, K. Peterson, and R. Fearing, "DASH: A dynamic 16g hexapedal robot,"

in *IEEE/RSJ International Conference on Intelligent Robots and Systems, 2009. IROS 2009*, 2009, pp. 2683–2689.

[7] A. Hoover and R. Fearing, "Fast scale prototyping for folded millirobots," in *IEEE International Conference on Robotics and Automation*. Citeseer, 2008, pp. 886–892.

[8] C.-S. Lin, C. Hwu, and W.-B. Young, "The thrust and lift of an ornithopter's membrane wings with simple flapping motion," *Aerospace Science and Technology*, vol. 10, no. 2, pp. 111 – 119, 2006.

[9] A. M. Mehta and K. S. J. Pister, "Warpwing: A complete open source control platform for miniature robots," in *submitted to IEEE/RSJ International Conference on Intelligent Robots and Systems, 2010.*, Oct. 2010.

[10] P. Holmes, D. Koditschek, and J. Guckenheimer, "The dynamics of legged locomotion: Models, analyses, and challenges," *Dynamics*, vol. 48, no. 2, pp. 207–304, 2006.

[11] J. Cham, S. Bailey, J. Clark, *et al.*, "Fast and robust: Hexapedal robots via shape deposition manufacturing," *The International Journal of Robotics Research*, vol. 21, no. 10-11, p. 869, 2002.

[12] S. Kim, J. Clark, and M. Cutkosky, "isprawl: Design and tuning for high-speed autonomous open-loop running," *The International Journal of Robotics Research*, vol. 25, no. 9, p. 903, 2006.

[13] J. Seipel, P. Holmes, and R. Full, "Dynamics and stability of insect locomotion: a

hexapedal model for horizontal plane motions," *Biological cybernetics*, vol. 91, no. 2, pp. 76–90, 2004.